Journal of Colloid and Interface Science 338 (2009) 428–434

Contents lists available at ScienceDirect

Journal of Colloid and Interface Science

www.elsevier.com/locate/jcis

Characterization of patterned poly(methyl methacrylate) brushes under various structures upon solvent immersion

Jem-Kun Chen [a,*], Chih-Yi Hsieh [b], Chih-Feng Huang [c], Po-min Li [b]

[a] Department of Polymer Engineering, National Taiwan University of Science and Technology, 43, Sec 4, Keelung Rd, Taipei, 106 Taiwan, People's Republic of China
[b] Department of Biomechatronics Engineering, National Pingtung University of Science and Technology, PingTung, Taiwan
[c] Department of Applied Chemistry, National Chiao Tung University, Hsinchu, Taiwan

ARTICLE INFO

Article history:
Received 28 April 2009
Accepted 17 June 2009
Available online 21 June 2009

Keywords:
ATRP
Grafting density
Surface coverage
Very-large-scale integration
PMMA brush

ABSTRACT

In this paper we describe a graft polymerization/solvent immersion method for generating various patterns of polymer brushes. We used a very-large-scale integration (VLSI) process and oxygen plasma system to generate well-defined patterns of polymerized methyl methacrylate (MMA) on patterned Si(1 0 0) surfaces through atom transfer radical polymerization (ATRP). After immersion of wafers presenting lines of these PMMA brushes in water and tetrahydrofuran, we observed mushroom- and brush-like regimes through grafting densities and surface coverages, respectively, for the PMMA brushes with various pattern resolutions. In the mushroom-like regime, the distance between lines of PMMA brushes was smaller than that of the lines patterned lithographically on the wafer; in the brush-like regime, this distance was approximately the same. This new strategy allows polymer brushes to be prepared through graft polymerization and then have their patterns varied through solvent immersion.

1. Introduction

In recent years, the preparation of polymer brushes has emerged as a robust method for creating surfaces exhibiting a wide range of mechanical and chemical properties; in many ways, they act as ideal alternatives to self-assembled monolayers (SAMs) [1–4]. Functionalization of silicon surfaces with organics is emerging as an important area in the development of new silicon-based devices, such as biomicroelectromechanical systems (BioMEMS), three-dimensional micro- and nanomemory chips, and DNA- and protein-based biochips and biosensors [5–8]. The use of polymers as building blocks for surface modification allows the preparation of "smart" or responsive surfaces based on conformational changes in the polymer backbones. These desirable traits have been manipulated in the areas of microelectronics and microfluidics [9].

Patterned polymer brushes are routinely produced from the initiator monolayer on a patterned surface [10–12]. Furthermore, micropatterned polymer brushes are of crucial importance to the development of biochips, microarrays, and microdevices for cell growth, regulation of protein adsorption, and drug delivery [13–15]. A variety of techniques, including microlithography [16] and chemical amplification of patterned monolayers from self-assembly [17,18] have been developed for fabricating patterned polymer brushes. The applicability of these patterned polymer films is restricted by their limited stability with respect to solvents and their tendency to undergo subsequent chemical reactions [19] as well as by difficulties in their preparation over large areas and complicated topographies.

One goal for the fabrication of patterned macromolecular architectures on surfaces is the realization of complex, often multimolecular, entities in which various interacting organic, biomolecular, and inorganic components are positioned in such a way as to give rise to unique properties and precisely defined structure-dependent functions. The generation of complex patterns in polymer films is traditionally achieved by using a combination of spin-casting and photolithographic techniques [20]. Current commercial lithographic processes can generate patterns with perfection over macroscopic areas and with dimensional control of features, registration, and overlay within tight tolerances and margins. In the past decade, considerable resources have been allocated to the development of exposure tools capable of resolving nanoscale patterns (<30 nm) with the required resolution and overlay capabilities, but relatively modest investments have been made for the development of suitable imaging materials on this length scale. Although these developments are continuing to push the limits of nano-manufacturing, the materials and processes themselves are not amenable to production purposes in their present form [21]. Self-assembling materials used in conjunction with the most advanced exposure tools may enable the current manufacturing practices to be extended to dimensions of 10 nm and less. In addition, Biggs et al. [22] reported the in situ observation of a relatively brush-like polymer structure using atomic force microscopy (AFM) and several reports have described the formation of

* Corresponding author. Fax: +886 2 27376544.
E-mail address: jkchen@mail.ntust.edu.tw (J.-K. Chen).

0021-9797/$ - see front matter © 2009 Elsevier Inc. All rights reserved.
doi:10.1016/j.jcis.2009.06.040

mushroom-like structures under various conditions [23,24]. Most of these studies have focused on changes in the thickness of the grafted layers; in contrast, the morphological changes of the surface structures in response to changes in solvent have not been characterized very well. In this paper, we report a program of research aimed at using polymerization to chemically amplify surfaces patterned with a VLSI system into patterned PMMA brushes. We have covalently bonded ATRP initiators onto hydroxylated surface patterns prepared using electron beam lithography and oxygen plasma treatment system, and then amplified the system vertically using ATRP. This surface-initiated polymerization process provides an avenue toward the rapid fabrication of high-resolution patterns of polymers. We observed distinct brush- and mushroom-like structures for PMMA brushes patterned with lines and dots after immersion in tetrahydrofuran (THF) and water.

2. Experimental

2.1. Materials

Single-crystal silicon wafers, Si(1 0 0), polished on one side (diameter: 6 in.) were supplied by Hitachi, Inc. (Japan) and cut into 2 cm × 2 cm samples. The materials used for graft polymerization, viz., (4-chloromethyl)phenyltrichlorosilane (CMPCS), methyl methacrylate (MMA), copper(I) bromide, and N, N, N′, N′, N″-pentamethyldiethylenetriamine (PMDETA), were purchased from Aldrich Chemical Co. MMA, PMDETA, and CMPCS were purified through vacuum distillation prior to use. All other chemicals and solvents were of reagent grade and purchased from Aldrich Chemical Co. All solvents were of reagent grade and used without further purification. To remove dust particles and organic contaminants, the Si surfaces were ultrasonically rinsed sequentially with methanol, acetone, and dichloromethane for 10 min each and subsequently dried under vacuum. The Si substrates were immersed in hydrofluoric acid solution (50 wt.%) for 5 min at room temperature to remove the silicon oxide film. The hydrofluoric acid-treated substrates were then immersed in the mixture of HNO_3 and H_2O_2 (2:1, mol%) for 10 min and subsequently rinsed with doubly distilled water a minimum of five times to oxidize the Si. This treatment process reduced the water contact angle of the surface from 45 ± 1° to 10 ±2° [25].

2.2. Immobilization of the initiator on the Si surface

The basic strategy for the fabrication of the patterned polymer brushes using the very-large-scale integration (VLSI) process is depicted in Fig. 1 and Scheme 1. The Si wafer was treated with hexamethyldisilazane (HMDS) in a thermal evaporator (Track MK-8) at 90 °C for 30 s to transform the hydroxyl groups on the surface of wafer into an inert film of $Si(CH_3)_3$ groups. The photoresist was spun on the HMDS-treated Si wafer at a thickness of 780 nm. Advanced lithography was then used to pattern the photoresist with an array of trenches and contact holes having dimensions between 200 nm and 10 μm after development. The sample was then subjected to oxygen plasma treatment (OPT) using a TCP 9400SE instrument (Lam Research Co, Ltd) to form hydroxyl groups from the HMDS-treated surface. Plasma treatment of the Si substrates was performed between two horizontal parallel plate electrodes (area: 12 cm × 12 cm). The plasma power supply was set to 300 W at a frequency of 13.5 MHz. The substrate was placed on the bottom electrode with the Si(1 0 0) surface exposed to the glow discharge at an oxygen pressure of ca. 5×10^{-3} torr for a predetermined period of time to form peroxide and hydroxyl peroxide species for the subsequent graft polymerization experiment [26]. Because the glow discharge chamber was purged thoroughly with a continuous oxygen stream prior to ignition, the residual air or water vapor in the chamber had negligible, if any, effect. Oxygen plasma treatment caused the surface to become chemically modified (strongly hydrophilic or polar) only in the areas not covered by the photoresist [27]. The introduction of these polar groups provided a more wettable surface for the preparation of the SAM monolayer for graft polymerization. To immobilize the ATRP initiator (CMPCS), the Si substrate treated with HMDS and oxygen plasma was immersed in a 0.5% (w/v) solution of CMPCS in toluene for 3 h at 50 °C. The CMPCS units assembled selectively onto the bare regions of the Si surface after oxygen plasma treatment, where it reacted with Si–O and Si–O–O species. This procedure resulted in a surface patterned with regions of CMPCS for ATRP and regions of photoresist. The functionalized Si substrates were removed from the solution, washed with toluene for 15 min to remove any unreacted material, dried under a stream of nitrogen, and subjected to surface-initiated polymerization reactions. Finally, the surfaces were dried under vacuum and stored in a dry nitrogen atmosphere.

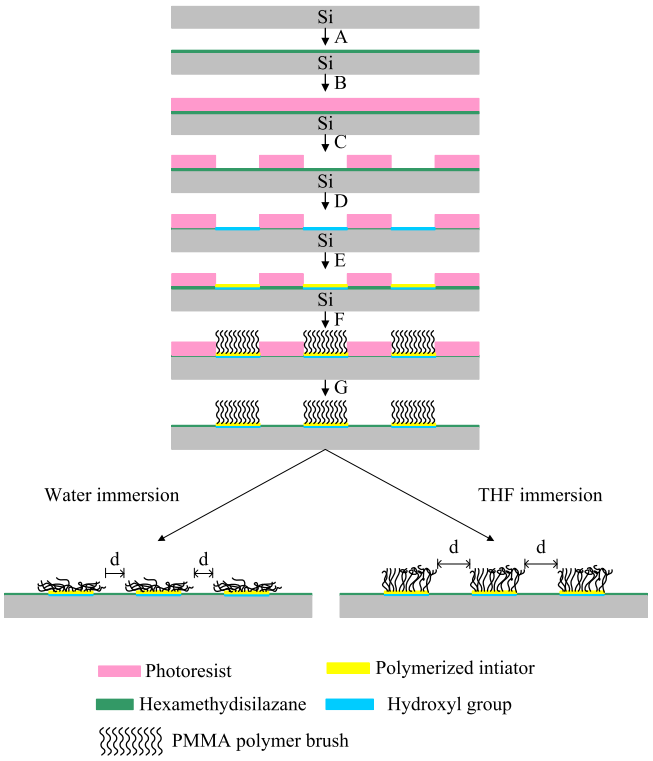

Fig. 1. Schematic representation of the process used to fabricate surfaces chemically nanopatterned with PMMA brush. (A) Silicon wafer is treated with HMDS in a thermal evaporator. (B) Photoresist is spin-coated onto the Si surface presenting $Si(CH_3)_3$ groups. (C) Advanced lithography is utilized to pattern the photoresist with arrays of trenches on the surface. (D) Oxygen plasma etching is used to chemically modify the exposed regions presenting $Si(OCH_3)_3$ groups and to convert the topographic photoresist pattern into a chemical surface pattern. (E) Initiator, CMPCS, is selectively assembled onto the bare regions of the Si surface. (F) Sample grafting proceeds via surface-initiated polymerization (ATRP) of MMA from the functionalized areas of the patterned SAM. (G) Photoresist is removed through treatment with a solvent.

2.3. Surface initiated atom transfer radical polymerization

For the preparation of PMMA brushes on the Si–CMPCS surface, MMA, Cu(I)Br, and PMDETA were added to anhydrous toluene. The solution was stirred and degassed with argon for 20 min. The Si–CMPCS substrate was then added to the solution and the temperature was raised to 85 °C. After various polymerization times, the wafers were placed in a Soxhlet apparatus to remove any

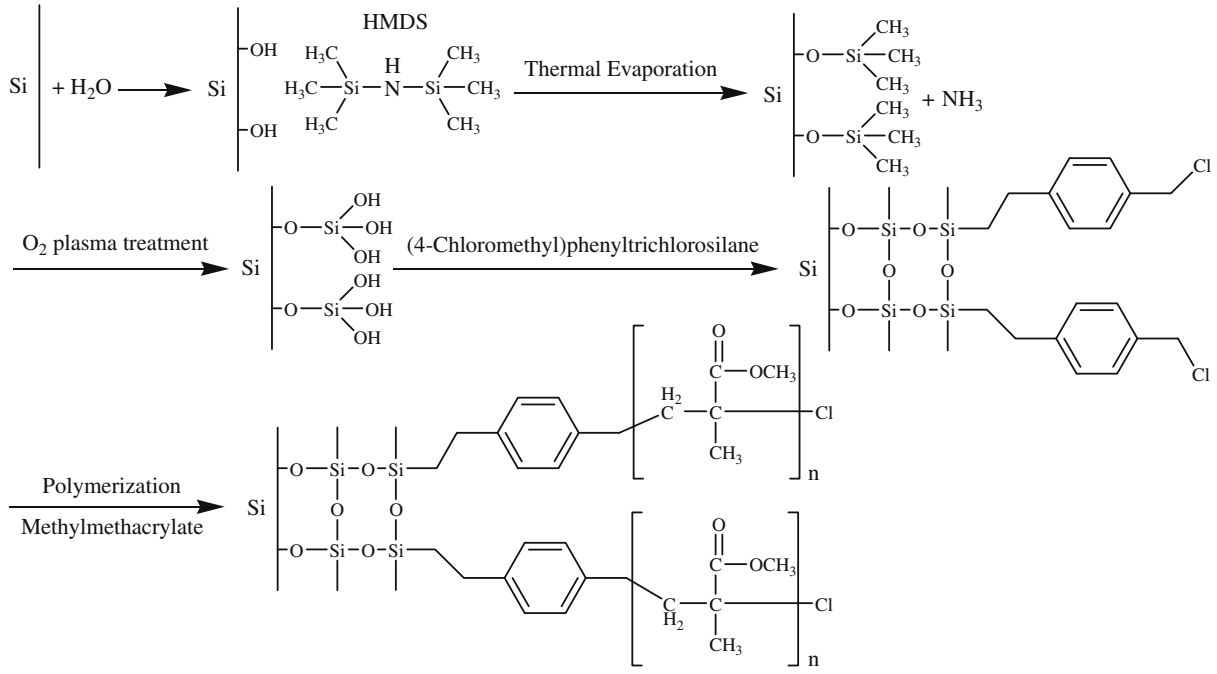

Scheme 1. Synthetic route toward PMMA brushes patterned through OPT, advanced lithography, and ATRP on Si wafers.

unreacted monomer, catalyst, and non-grafted material. The remaining photoresist was removed from the HMDS-treated surface by rinsing with solvent, leaving behind the chemically nanopatterned surface. The surfaces were then dried under vacuum at 80 °C for 20 min. The PMMA brushes were immersed in water and tetrahydrofuran (THF) (poor and good solvent for PMMA, respectively) and treated ultrasonically for 3 h before drying under a stream of nitrogen. In addition, samples of "free" PMMA were synthesised in solution under the same conditions as those used for grafting polymerization to provide polymers having the same molecular weights of PMMA as the brushes grafted on the Si surface. The "free" PMMA generated in solution from the sacrificial initiator was recovered through precipitation of the reaction mixture into methanol; it was analyzed using gel permeation chromatography (GPC). The monomer conversion was determined gravimetrically. GPC measurements were performed using a VISCOTEK-DM400 instrument and a LR 40 refractive index detector. THF was used as the mobile phase for PMMA; THF containing triethylamine (2 vol.%) was used as the mobile phase for PDMAEMA.35 Monodisperse polystyrene standards (Polymer Lab, Agilent Co.) were used to generate the calibration curve. Although the exact molecular weight of the polymer grafted on the Si surface is not known, the molecular weight of the graft polymer was expected to be proportional to that of the polymer formed in the solution [28]. The polymer-modified Si surfaces were analyzed using ellipsometry (SOPRA SE-5, France), X-ray photoelectron spectroscopy (XPS; PHI 1600 Physical Electronics, USA), a contact angle system (Krüss gmbh, Germany), and AFM (Veeco Dimension 5000 Scanning Probe Microscope).

3. Results and discussion

3.1. Characterization of the Si surface for PMMA brushes

To prepare polymer brushes on the Si surface, it was necessary for us to immobilize a uniform and dense layer of initiators on the Si surface. The chemical compositions of the pristine Si(1 0 0) surface and the Si surfaces at various stages during the surface modification process were determined using XPS through C/Si and O/Si ratio with considerable inaccuracy as shown in Fig. 2. Two peak components at the binding energies (BE) of ca. 99 and 103 eV, attributable to Si–Si and Si–O species, respectively, appear in the Si 2p core-level spectrum of the pristine Si(1 0 0) surface [29]. Treatment of the pristine Si(1 0 0) surface with HMDS passivated the native oxide layer and yielded a Si–C surface. Treatment of the Si surface with oxygen plasma removed the Si–C layer to activate the Si surface with Si–O species, which decreased the C/Si ratio and increased the O/Si ratio. The C/Si ratio from C 1s core-level spectrum of the initiator (CMPCS)-functionalized Si surface, curve-fitted with two peak components having BEs at ca. 283.9 and 284.6 eV, increased significantly because of the presence of C–H species of the CMPCS layer on the surface. [29] Additionally, the presence in the Cl 2p core-level spectrum of a signal at a BE of ca. 201.2 eV for the CMPCS-functionalized Si surface indicated that the CMPCS species had been immobilized successfully on the Si surface. Plasma is used extensively for the treatment of Si wafers, especially for surface cleaning and etching. The idea behind the

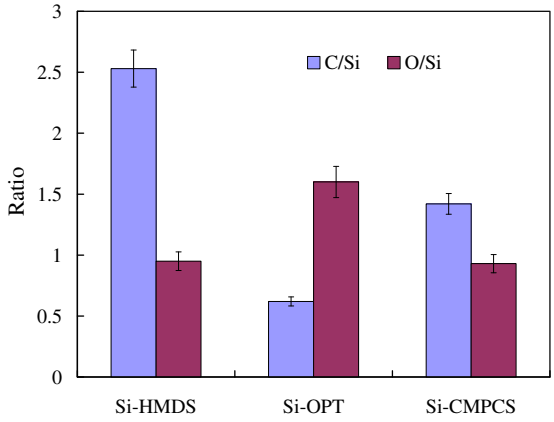

Fig. 2. Changes in the O/Si and C/Si atomic ratios with considerable inaccuracy of the Si–HMDS, Si–OPT and Si–CMPCS surface in the process.

utilization of the plasma is to create a very reactive gas environment enclosed in a vacuum. Surfaces in contact with the plasma experience interactions that may result in sputtering and chemical reactions caused by highly reactive radicals, low-energy ions, and electrons created in the plasma. Because the chemical properties of Si resemble those of carbon, it can be deduced that OPT of a Si surface, followed by atmospheric exposure, can also introduce some active oxygen species, such as the Si–O and Si–O–O units, that increase the O/Si ratio [30]. We used these active oxygen species for reactions with the initiator of graft polymerization in the subsequent experiments. The introduction of polar groups through plasma treatment also provided a more wettable surface, which the contact angle for water decreased rapidly during OPT up to a treatment time of ca. 5 s.

In pervious study, we used XPS analysis to investigate the presence of grafted PMMA brushes on the Si surface [29]. We obtained from XPS analysis of the Si–CMPCS–PMMA surface are in fairly good agreement with the respective theoretical ratios. Otherwise, the results displayed the thicknesses of the PMMA brushes grafted for various times onto the Si–CMPCS surfaces, recorded after ultrasonication in water or THF for 3 h. These observations revealed that the PMMA brushes formed mushroom- and brush-like regimes after immersion in water and THF, respectively. In addition, we obtained the linear relationship between $\ln([M_0]/[M])$ and time, where $[M_0]$ is the initial monomer concentration and $[M]$ is the monomer concentration. The concentration of the growing species remained constant, and first-order kinetics were obtained [29]. The number-average molecular weight of the "free" PMMA increased linearly upon increasing the monomer conversion. The polydispersity index (PDI, M_w/M_n) of the free PMMA was ca. 1.2. Although we did not determine the exact molecular weight of the polymer grafted on the Si surface, we expected the molecular weight of the graft polymer to be proportional to that of the polymer formed in solution; i.e., we expected the molecular weight of the "free" PMMA formed in the solution to increase linearly with respect to the thickness of the PMMA brushes for various polymerization times. The grafting density in chains per surface area (D_s, chains/nm^2) is calculated according to the equation

$$D_s = ThdN_a/M_n$$

where M_n is the molecular weight (g/mol), Th is the thickness (nm), d is the density (g/nm^3), N_a is Avogadro's number (molecules/mol), and a density of 1.18×10^{-21} g/nm^3 for bulk PMMA. Fig. 3 displays the grafting density (D_s) with considerable inaccuracy of the graft polymerization onto the Si–CMPCS surfaces, recorded after ultrasonication in water and THF for 3 h. The approximately linear increases was observed in grafting densities of the grafted PMMA layer upon polymerization time increasing to 8 h, after immersion in THF. The grafting densities reached a plateau, indicating the formation of brush-like regime of the PMMA brushes, after good solvent (THF) immersion of the polymer obtained after 8 h of polymerization time. However, the grafting densities of the PMMA brushes grafted on the Si substrate after water immersion demonstrated a maximum value at 8 h polymerization time, but decreased as the polymerization time more than 8 h. The observation suggested that the PMMA brushes after water immersion collapsed to fill the defect area on the surface as the polymerization time more than 8 h of polymerization time, causing the decrease of the grafting density. The surface coverage, defined as the amount of the grafted polymer per square meter of surface, is calculated from the product of the thickness and the density of the grafted polymer layer.

$$\text{Surface coverage} = \text{film thickness} \times \text{density}$$

For simplicity, we used the density of the corresponding bulk polymer (1.18 g/cm^3 for PMMA) as the density of the grafted polymer film. Fig. 4 displays the surface coverage (mg/m^2) with considerable inaccuracy resulting from the ill-defined heights of the PMMA brushes grafted for various times onto the Si–CMPCS surfaces, recorded after ultrasonication in water or THF for 3 h. The approximately linear increases in surface coverage of the grafted PMMA layer on the Si–CMPCS surface upon increasing the polymerization time to 12 h, after immersion in either water or THF. The surface coverage reached a plateau, indicating extension of the PMMA brushes into a brush-like regime, after poor solvent (water) immersion of the polymer obtained after polymerization for more than 12 h. In contrast, the surface coverage of the PMMA brushes grafted on the Si substrate after THF immersion continued to increase upon increasing the polymerization time beyond 12 h, providing a brush-like regime of PMMA brushes. These observations reveal that the PMMA brushes formed mushroom- and brush-like regimes after immersion in water and THF, respectively. These two coverages represent the two types of regimes formed from the PMMA brushes immersed in the poor and good solvents. For the Si–CMPCS–PMMA surface, the surface coverage is comparable to that reported previously for PMMA brushes grown from a native (oxide-covered) Si surface via ATRP [30]. Our calculated

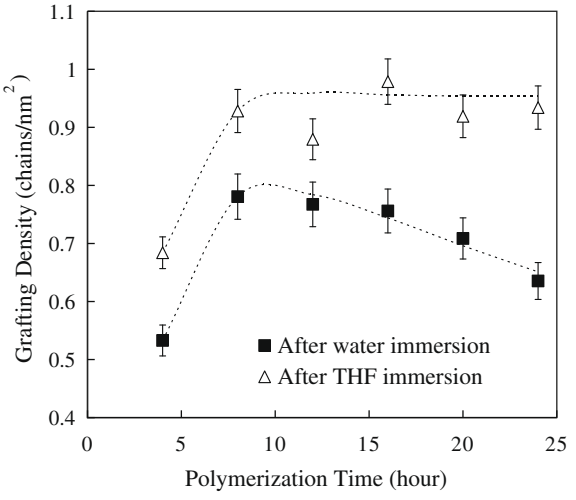

Fig. 3. Dependence of the grafting density in chains per surface area (D_s, chains/nm^2) of the PMMA layer, grown from the Si–CMPCS surface via ATRP and then immersed in water or THF, on the polymerization time.

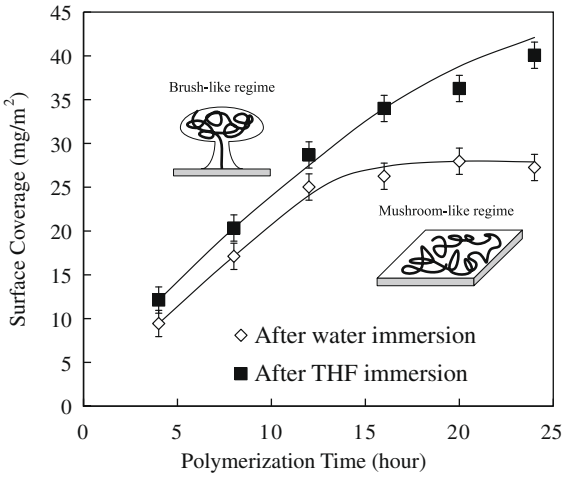

Fig. 4. The surface coverage (mg/m^2) of the PMMA layer, grown from the Si–CMPCS surface via ATRP and then immersed in water or THF, as a function of the polymerization time.

grafting densities and surface coverages verified the structural change of the PMMA brushes from the brush- to mushroom-like regimes in water and THF, respectively. These results obtained after solvent immersion indicate that the process of surface-initiated ATRP of MMA is controlled between two regimes for PMMA brushes. In addition, the collapsed point, transition of the two regimes, corresponding to the polymerization time for grafting density and surface coverage are 8 h and 12 h, respectively. The deviation of the collapsed point in water immersion system for grafting density and surface coverage is caused by the considerable inaccuracy from thickness measurement. The results suggests that the PMMA layer after water immersion formed the brush- or mushroom-like regime when the polymerization time was between 8 and 12 h, corresponding the ca. 20 nm of thickness for the collapsed point of PMMA brushes.

3.2. Surface morphology and patterned PMMA brushes

The root-mean-square surface roughness (R_a) of the pristine Si–H surface was only ca. 0.42 nm. The Si–HMDS and Si–OPT surfaces remained molecularly uniform with values of R_a of ca. 0.51 and 0.55 nm, respectively. After surface treatment with CMPCS, the R_a increased slightly to ca. 1.2 nm. In addition, ellipsometry data indicated that the grafted PMMA film exhibited nanoscopic uniformity in thickness.

These results suggest that ATRP graft polymerization proceeded uniformly on the Si–CMPCS surface to give rise to a dense coverage of PMMA. Lithography processes with positive photoresists were used to fabricate trenches (duty ratio = 1:1). The PMMA brushes were grafted from the Si–CMPCS surfaces of trenches to form lines of PMMA brushes. We used AFM to visualize the topographies of the patterned PMMA brushes grafted onto the Si surfaces through ATRP for 24 h and then subsequently immersed in water and THF. Fig. 5a and b presents representative AFM images of the patterned lines of PMMA brushes grafted for 24 h from trenches having a resolution of 5 μm and then immersed in water and THF, respectively. Fig. 5a reveals that the MMA polymer chains grafted for 24 h on the Si surface existed as a distinctive overlayer after immersion in water. The surface possessed the mushroom-like structure because of the isotropic or nematic collapse of the PMMA brushed in the presence of the poor solvent [31,32]. The formation of the islands in Fig. 5b probably resulted from the brush-like regime of the PMMA brushes in THF after they had been grafted for 24 h. The values of R_a of the PMMA brushes in their mushroom- and brush-like regimes were 2.876 and 6.758 nm, respectively. The width of the PMMA brushes after immersion in water and THF extended obviously over 5 μm and closed to 5 μm, respectively. These results confirm the success of the chemical amplification of the patterned hydroxyl-functionalized SAM into spatially localized polymer brushes. Because of the presence of the mushroom- and brush-like regimes, the widths of the trenches functionalized with PMMA brushes had different resolutions after immersion in water and THF, respectively. Fig. 6a presents SEM images of the patterned lines of PMMA brushes grafted for 24 h from trenches having a resolution of 3 μm. The PMMA brushes demonstrated a collapsed structure under vacuum system in the SEM chamber. The mushroom-like structure was observed obviously on the surface of the patterned PMMA brushes, causing the expansion of the PMMA brush resolution over 3 μm. The mushroom-like structure was

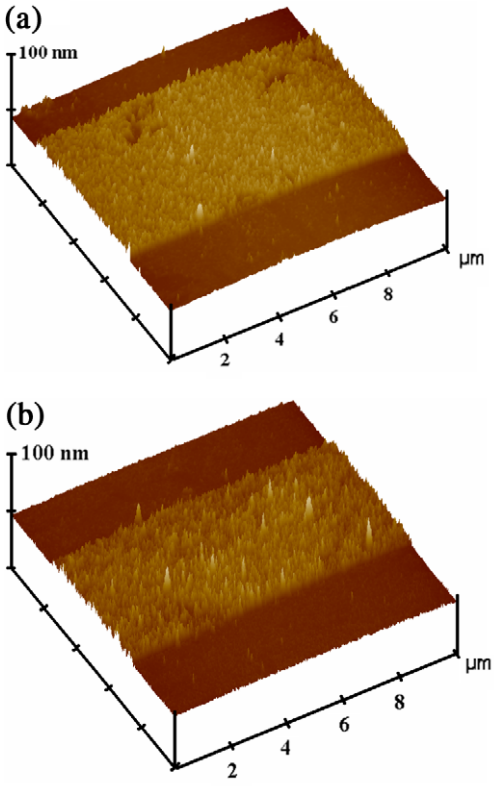

Fig. 5. AFM images of PMMA brushes (a, b) obtained after graft polymerization from 5-μm trenches for 24 h and immersion in (a) water and (b) THF.

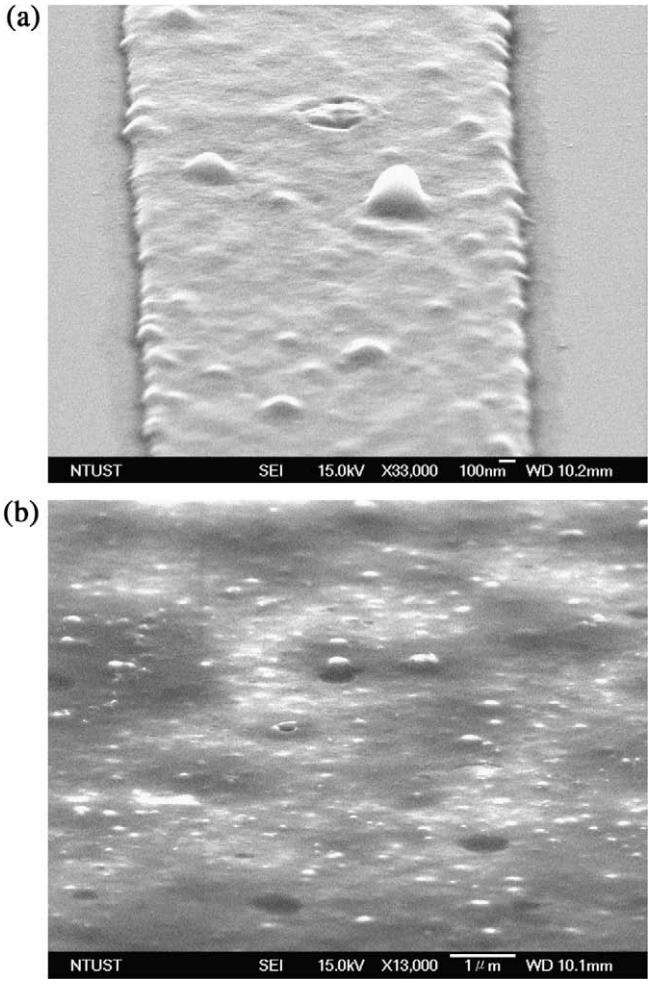

Fig. 6. SEM images of (a) PMMA brushes obtained after graft polymerization from 3-μm trenches for 24 h of polymerization time and (b) PMMA brush thin film on the silicon surface.

formed on the PMMA brush layer with radius of 100–300 nm due to the entanglement between the polymer chains under vacuum state. The observation suggests that the PMMA brushes demonstrated the various structures under atmospheric state and vacuum state, which observed by AFM and SEM system, respectively.

We used lithography processes with positive photoresists to fabricate trenches and contact holes (duty ratio = 1:1) with resolutions ranging from 200 nm to 10 μm. The PMMA brushes were grafted from the Si–CMPCS surfaces of trenches and contact holes to form lines and dots of PMMA brushes. The formed lines and dots of PMMA brushes with resolution from 200 nm to 700 nm and 200 nm to 5 μm, respectively, demonstrated unobvious patterns, ascribed to the few grafted site on the surface. Fig. 7 illustrated that the PMMA brushes grafted from various width trench of lithography pattern, causing the various thickness with considerable inaccuracy resulting from the ill-defined heights of the PMMA brushes. The thickness reached a plateau, indicating the formation of the PMMA brushes under rich grafted site as the lithography pattern over about 5 μm. These results suggest that the resolution of the grafted PMMA brushes corresponded to the grafted site on the surface. We compared the distances between the PMMA brushes (d, Fig. 1) after immersion in water and THF in relation to the original distances patterned by the lithography system. The trench distances between the PMMA brushes after water and THF immersion increased linearly with respect to the polymerization time (Fig. 8a) with considerable inaccuracy resulting from the ill-defined edges of the PMMA brushes. After water immersion, we observed that the PMMA brushes extended laterally upon increasing the polymerization time, causing the trench distances to shrink to below a duty ratio of 1:1. These results were consistent with the formation of the mushroom-like regime for the PMMA brushes after immersion in water. In contrast, the trench distances between the PMMA brushes after immersion in THF remained almost constant, consistent with the formation of the brush-like regime of the PMMA brushes after their immersion in the good solvent. Thus, our PMMA brushes exhibit various thicknesses and trench distances after immersion in good and poor solvents, providing mushroom- and brush-like regimes, respectively. The shrinkage (d' = lithography pattern width − d), which occurred under the various structure of PMMA brush after immersion in good and poor solvent, increased with the lithography pattern width (Fig. 8b) due to the various thicknesses of PMMA brushes under various grafted site density, corresponding to the results in Fig. 7. The shrinkage reached a plateau, indicating the formation of the PMMA brushes as the lithography trench width over about 5 μm for the rich grafted site.

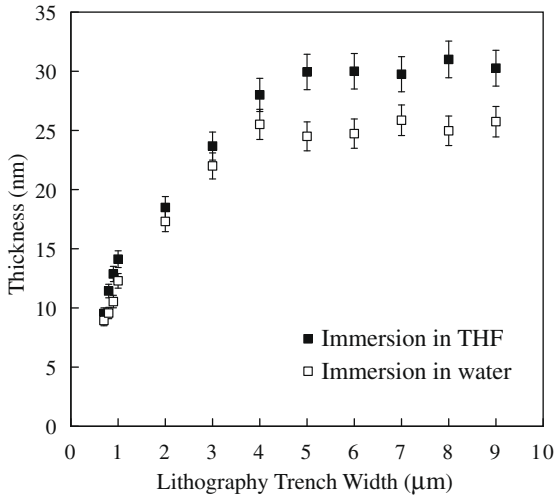

Fig. 7. Dependence of the thickness of the PMMA layer, grown from the trench of Si–CMPCS surface via ATRP and then immersed in water or THF, on the lithography trench width.

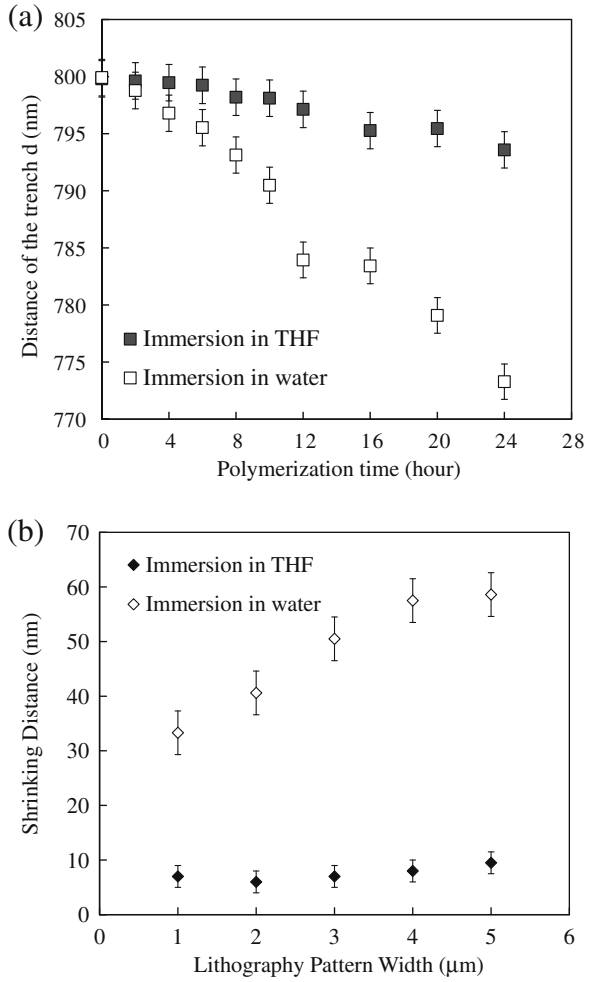

Fig. 8. (a) Relationship between the polymerization time of the PMMA brushes and the distance between PMMA brushes grafted from a 800-nm-wide trench under a duty ratio of 1:1 and then immersed in water and THF. (b) Dependence of the shrinkage (d' = lithography pattern width − d) on the lithography trench width.

4. Conclusion

We have developed a novel strategy for the preparation of patterned polymer brushes from Si surfaces using commercial semiconductor processes. The key feature is the use of surface-initiated polymerization after oxygen plasma treatment to chemically amplify a patterned SAM into a macromolecular film of PMMA. The patterned PMMA brushes exhibit mushroom- and brush-like regimes after immersion in poor (water) and good (THF) solvents, respectively, allowing the line widths of the PMMA brushes and the trench widths between them to be varied. We are at present extending this strategy to other polymer brushes and exploring the physical properties of these novel thin films.

References

[1] W. Senaratne, L. Andruzzi, C.K. Ober, Biomacromolecules 6 (2005) 2427.
[2] F. Zhou, W.T.S. Huck, Phys. Chem. Chem. Phys. 8 (2006) 3815.
[3] G.K. Jennings, E.L. Brantley, Adv. Mater. 16 (2004) 1983.
[4] Chia-Hao Chan, Jem-Kun Chen, Feng-Chih Chang, Sens. Actuators, B 13 (2008) 3327.
[5] S. Lan, M. Veiseh, M. Zhang, Biosens. Bioelectron. 20 (2005) 1697.

[6] F.J. Xu, S.P. Zhong, L.Y.L. Yung, E.T. Kang, K.G. Neoh, Biomacromolecules 5 (2004) 2392.
[7] Jem-Kun Chen, Chia-Hao Chan, Feng-Chih Chang, Appl. Phys. Lett. 92 (2008) 053108.
[8] S.E. Létant, B.R. Hart, S.R. Kane, M.Z. Hadi, J.G. Reynolds, Adv. Mater. 16 (2004) 689.
[9] R. Dong, S. Krishnan, B.A. Baird, M. Lindau, C.K. Ober, Biomacromolecules 8 (10) (2007) 3082.
[10] U. Schmelmer, R. Jordan, W. Geyer, W. Eck, A. Golzhauser, M. Grunze, A. Ulman, Angew. Chem., Int. Ed. 42 (2003) 559.
[11] I.S. Maeng, J.W. Park, Langmuir 19 (2003) 4519.
[12] M. Kaholek, W.K. Lee, S.J. Ahn, H. Ma, K.C. Caster, S. Zauscher, Nano Lett. 4 (2004) 373.
[13] L. Andruzzi, W. Senaratne, A. Hexemer, E.D. Sheets, S.B. Ilic, J.K. Kramer, B. Baird, C.K. Ober, Langmuir 21 (2005) 2495.
[14] T. Waku, M. Matsusaki, T. Kaneko, M. Akashi, Macromolecules 40 (17) (2007) 6385.
[15] L. Chen, D.J. Hook, P.L. Valint, J.A. Gardella, J. Vac. Sci. Technol. 26 (4) (2008) 616.
[16] L. Chen, L. Zhuang, P. Deshpande, S. Chou, Langmuir 21 (2005) 818.
[17] H.P. Brack, C. Padeste, M. Slaski, S. Alkan, H.H. Solak, J. Am. Chem. Soc. 126 (2004) 1004.
[18] S.J. Ahn, M. Kaholek, W.K. Lee, B. LaMattina, T.H. LaBean, S. Zauscher, Adv. Mater. 16 (2004) 2141.
[19] R. Zerushalmi-Royen, J. Klein, L. Fetters, Science 263 (1994) 793.
[20] M. Kaholek, W.K. Lee, J.X. Feng, B. LaMattina, D.J. Dyer, S. Zauscher, Chem. Mater. 18 (16) (2006) 3660.
[21] K.E. Gonsalves, L. Merhari, H. Wu, Y. Hu, Adv. Mater. 13 (2001) 703.
[22] N. Ishida, S. Biggs, Langmuir 23 (2007) 11083.
[23] C. Ohe, Y. Goto, M. Noi, M. Arai, H. Kamijo, K. Itoh, J. Phys. Chem. B 111 (2007) 1693.
[24] N. Ishida, S. Biggs, Macromolecules 40 (2007) 9045.
[25] J.K. Chen, F.H. Ko, K.F. Hsieh, C.T. Chou, F.C. Chang, J. Vac. Sci. Technol., B 22 (2006) 3233.
[26] D.P. Wu, B.X. Zhao, Z.P. Dai, J.H. Qin, B.C. Lin, Lab Chip 6 (7) (2006) 942.
[27] M.P. Stoykovich, M. Müller, S.O. Kim, H.H. Solak, E.W. Edwards, J.J. de Pablo, P.F. Nealey, Science 308 (2005) 1442.
[28] M. Ejaz, S. Yamamoto, K. Ohno, Y. Tsujii, T. Fukuda, Macromolecules 31 (1998) 5934.
[29] Jem-Kun Chen, Chih-Yi Hsieh, Chih-Feng Huang, Po-Min Li, Shiao-Wei Kuo, Feng-Chih Chang, Macromolecules 41 (2008) 8729.
[30] H. Mori, A. Boker, G. Krausch, A.H.E. Muller, Macromolecules 34 (2001) 6871.
[31] M.D. Rowe-Konopacki, S.G. Boyes, Macromolecules 40 (2007) 879.
[32] B. Zhao, W.J. Brittain, Prog. Polym. Sci. 25 (2000) 677.